Radiation-induced second primary cancer risks from modern external beam radiotherapy for early prostate cancer: impact of stereotactic ablative radiotherapy (SABR), volumetric modulated arc therapy (VMAT) and flattening filter free (FFF) radiotherapy

You may also be interested in:

A critical evaluation of secondary cancer risk models applied to Monte Carlo dose distributions of 2-dimensional, 3-dimensional conformal and hybrid intensity-modulated radiation therapy for breast cancer
A Joosten, F Bochud and R Moeckli

Second cancer risk following radiotherapy
R Takam, E Bezak and E E Yeoh

The risk of radiation-induced second cancers in the high to medium dose region: a comparison between passive and scanned proton therapy, IMRT and VMAT for pediatric patients with brain tumors
Maryam Moteabbed, Torunn I Yock and Harald Paganetti

Risk of radiogenic second cancers following volumetric modulated arc therapy and proton arc therapy for prostate cancer
Laura A Rechner, Rebecca M Howell, Rui Zhang et al.

Stray photon dose following flattening filter removal
Stephen F Kry, Oleg N Vassiliev and Radhe Mohan

Risk-optimized proton therapy to minimize radiogenic second cancers
Laura A Rechner, John G Eley, Rebecca M Howell et al.

Organ-specific radiation-induced cancer risk estimates due to radiotherapy for benign pigmented villonodular synovitis
Michalis Mazonakis, Antonis Tzedakis, Efrossyni Lyraraki et al.

Variability of a peripheral dose among various linac geometries for second cancer risk assessment
A Joosten, F Bochud, S Baechler et al.

Radiation-induced second primary cancer risks from modern external beam radiotherapy for early prostate cancer: impact of stereotactic ablative radiotherapy (SABR), volumetric modulated arc therapy (VMAT) and flattening filter free (FFF) radiotherapy

Louise J Murray[1,3]**, Christopher M Thompson**[2]**, John Lilley**[2]**, Vivian Cosgrove**[2]**, Kevin Franks**[1]**, David Sebag-Montefiore**[1,3] **and Ann M Henry**[1]

[1] Department of Clinical Oncology, Institute of Oncology, Leeds Cancer Centre, St James's University Hospital, Beckett St, Leeds LS9 7TF, UK
[2] Department of Medical Physics, Institute of Oncology, Leeds Cancer Centre, St James's University Hospital, Beckett St, Leeds LS9 7TF, UK
[3] University of Leeds, Leeds LS2 9JT, UK

E-mail: Ann.Henry@leedsth.nhs.uk

Abstract

Risks of radiation-induced second primary cancer following prostate radiotherapy using 3D-conformal radiotherapy (3D-CRT), intensity-modulated radiotherapy (IMRT), volumetric modulated arc therapy (VMAT), flattening filter free (FFF) and stereotactic ablative radiotherapy (SABR) were evaluated. Prostate plans were created using 10 MV 3D-CRT (78 Gy in 39 fractions) and 6 MV 5-field IMRT (78 Gy in 39 fractions), VMAT (78 Gy in 39 fractions, with standard flattened and energy-matched FFF beams) and SABR (42.7 Gy in 7 fractions with standard flattened and energy-matched FFF beams). Dose-volume histograms from pelvic planning CT scans of three prostate patients, each planned using all 6 techniques, were used to calculate organ equivalent

doses (OED) and excess absolute risks (EAR) of second rectal and bladder cancers, and pelvic bone and soft tissue sarcomas, using mechanistic, bell-shaped and plateau models. For organs distant to the treatment field, chamber measurements recorded in an anthropomorphic phantom were used to calculate OEDs and EARs using a linear model. Ratios of OED give relative radiation-induced second cancer risks.

SABR resulted in lower second cancer risks at all sites relative to 3D-CRT. FFF resulted in lower second cancer risks in out-of-field tissues relative to equivalent flattened techniques, with increasing impact in organs at greater distances from the field. For example, FFF reduced second cancer risk by up to 20% in the stomach and up to 56% in the brain, relative to the equivalent flattened technique. Relative to 10 MV 3D-CRT, 6 MV IMRT or VMAT with flattening filter increased second cancer risks in several out-of-field organs, by up to 26% and 55%, respectively. For all techniques, EARs were consistently low. The observed large relative differences between techniques, in absolute terms, were very low, highlighting the importance of considering absolute risks alongside the corresponding relative risks, since when absolute risks are very low, large relative risks become less meaningful.

A calculated relative radiation-induced second cancer risk benefit from SABR and FFF techniques was theoretically predicted, although absolute radiation-induced second cancer risks were low for all techniques, and absolute differences between techniques were small.

(Some figures may appear in colour only in the online journal)

1. Introduction

The development of a radiation-induced second primary cancer is an unwanted consequence of radiotherapy treatment. Theoretical concerns have been raised that modern techniques such as intensity-modulated radiotherapy (IMRT) may increase second cancer risk (Hall and Wuu 2003). Owing to the relative newness of IMRT compared to the latency of second primary cancers, the clinical evidence regarding the impact of modern radiotherapy techniques on radiation-induced second cancer risk is too immature to determine if these concerns are warranted (Huang *et al* 2011, Zelefsky *et al* 2012a, 2012b). While radiation-induced second cancer risk from IMRT has been compared to that from 3D-conformal radiotherapy (3D-CRT) in prostate planning studies (Followill *et al* 1997, Kry *et al* 2005a, 2005b, Stathakis *et al* 2007, Ruben *et al* 2008, Bednarz *et al* 2010), far fewer comparisons with other techniques such as volumetric modulated arc therapy (VMAT) (Rechner *et al* 2012), stereotactic ablative radiotherapy (SABR) (Dasu *et al* 2011) and flattening filter free (FFF) techniques (Kry *et al* 2010, Halg *et al* 2012) have been performed.

This study aimed to compare radiation-induced second cancer risk from modern radiotherapy techniques used to treat early prostate cancer. Conventionally fractionated schedules using 3D-CRT, IMRT and VMAT with standard (flattened) and FFF beams were evaluated, together with SABR using VMAT with standard and FFF beams.

2. Methods

2.1. Contouring

Pelvic CT scans which were previously used for radiotherapy planning for three early stage prostate cancer patients were selected at random. On each of these, the, CTV was defined as the prostate alone, expanded 6 mm to PTV (compatible with daily online imaging using fiducial markers (Adamson *et al* 2011, Quon *et al* 2012, Beltran *et al* 2008). The rectum (recto-sigmoid junction to anus), bladder and femoral heads were contoured as organs-at-risk. A 5 mm shrink margin was created within the bladder and the subtraction of this from the whole bladder represented the bladder wall. Patients had empty rectums, thus the whole rectal volume represented rectal dose (since total rectal volume is considered a suitable surrogate for the rectal wall if the rectum is empty (Fiorino *et al* 2009)). All pelvic bones were contoured.

2.2. Planning

Five plans were produced for each pelvic CT using Monaco v3.3 (Elekta, AB Sweden) with a Monte Carlo algorithm, 6 MV photons, a 2 mm grid and the Agility head (Elekta, AB Sweden). A 5-field step and shoot IMRT plan was produced, prescribed 78 Gy in 39 fractions, with beams at 180°, 252°, 324°, 36° and 108°. Two VMAT plans prescribed 78 Gy in 39 fractions were produced using one 240° arc (240 ° → 120 °), one with a 6 MV beam and one with an energy-matched 6 MV FFF beam. Two SABR plans prescribing 42.7 Gy in 7 fractions were produced, using one 240° VMAT arc (240 ° → 120 °), with 6 MV and energy-matched 6 MV FFF beams. 'Energy-matched' means the FFF beam energy was re-tuned to match the relative dose in water at 10 cm deep for a 10 × 10 cm standard 6 MV beam, 100 cm SSD (Paynter *et al* 2014). Doses were prescribed so that ≥95% of the PTV received ≥95% of the prescription dose and median dose was within 1 Gy of the prescription dose. Organ-at-risk constraints are described in table 1.

3D-CRT plans cannot be produced using Monaco v3.3.A 10 MV 3D-CRT four-field (0°, 180°, 90°, 270°) 78 Gy in 39 fraction plan was therefore produced using Oncentra MasterPlan (Elekta, AB Sweden). Here, the prescription dose was normalized to the centre of the PTV and the 95% isodose covered the PTV (aiming for 100% coverage, accepting ≥95%).

2.3. In-field and close-to-field second cancer risk assessment

Differential dose-volume histograms (DVHs) using 0.01 Gy bin widths for rectum, bladder wall, pelvic bones and pelvic soft tissue (total scanned volume minus bones and prostate) were exported and used to calculate organ equivalent dose (OED) and excess absolute risk (EAR) for second rectal and bladder cancers, as well as bone and soft tissue sarcomas within the scanned volume, for all three pelvic CT scans and all six techniques, as described below. Average values are presented.

2.4. Out-of-field second cancer risk assessment

All six techniques from one of the three pelvic CT scans were delivered to the RANDO® phantom (The Phantom Laboratory, USA) to assess out-of-field doses. Plans were delivered using a Synergy linac (Elekta, AB Sweden) with the Agility head (Elekta, AB Sweden) with and without FFF high dose rate mode. For conventionally fractionated treatments, three 2 Gy fractions were delivered. For each SABR plan, one 6.1 Gy fraction was delivered. Measurements were performed in the midline at increasing distances from the isocentre by substituting each

Table 1. Organ-at-risk constraints.

	78 Gy in 39 fraction constraints	Source	SABR constraints	Source
Rectum	V70 Gy(90%) < 15% V59 Gy(76%) < 35% V51 Gy(65%) < 45%	HYPO-PR-RT trial (Franzen and Widmark 2011)	V41.4 Gy(97%) < 3% V38.4 Gy(90%) < 15% V32.0 Gy(75%) ≤ 35% V28.0 Gy(65%) ≤ 45% V24.8 Gy(58%) < 70% V19.6 Gy(46%) < 80%	HYPO-PC RT trial (Franzen and Widmark 2011) plus biologically equivalent constraints to 74 Gy arm of CHHiP trial for high and low dose regions (Dearnaley 2010)
Bladder	V80 Gy(103%) < 15% V75 Gy(96%) < 25% V70 Gy(90%) < 35% V65 Gy(83%) < 50%	RTOG 0126 (Radiation Therapy Oncology Group 2014)	V41.4 Gy(97%) < 5% V34.7 Gy(81%) < 25% V29.9 Gy(70%) < 50%	Biologically equivalent constraints to 74 Gy arm of CHHiP trial (Dearnaley 2010)
Femoral heads	Dmax ≤ 55 Gy(70%)	HYPO-PR-RT trial (Franzen and Widmark 2011)	Dmax ≤ 29.9 Gy(70%)	HYPO-PC RT trial (Franzen and Widmark 2011)

relevant phantom slice for a 2.5 cm tall Perspex block with an ionization chamber holder, such that measurements were performed at approximately midline depth (figure 1). Doses at specific distances from the isocentre were taken to represent doses received by organs located at approximately those positions (table 2).

Out-of-field measurements were performed using a semi-flex ionization chamber (PTW GmbH, Germany), calibrated for 6 MV, 6 MV FFF and 10 MV beams. In other studies, thermoluminescent dosimeters (TLD) have often been used for out-of-field measurements given their relative energy independence. TLDs, however, can prove difficult in terms of accuracy and reproducibility, with uncertainties up to 10% quoted (Kragl *et al* 2011). The concern regarding chamber out-of-field measurements is the lower energy spectra in this region. It has been demonstrated, however, that the mean energy spectra out to 20 cm from the field edge are in the kilovoltage range (Kragl *et al* 2011), within the range of use of the chosen chamber. At 10–20 cm from the field edge, it appears the energy spectra are plateauing or at worst decreasing gradually (Kragl *et al* 2011), thus providing confidence in performing measurements at 20 cm and beyond. In keeping with out-of-field chamber measurements performed by others, we assumed 5% uncertainty to account for potential inaccuracies resulting from the MV calibrated ion chamber and positioning inaccuracies (Kragl *et al* 2011). Readings were corrected for temperature, pressure and leakage. To estimate the impact of drift on measurements, on the first full day of measurements, we positioned a second semi-flex chamber at 70 cm from the isocentre and doses were recorded here at the same time as recording measurements at points closer to the isocentre (figure 1). At 70 cm, where the impact of drift was assumed to be greatest, the average standard deviation was 2.57% of the mean reading at 70 cm. Drift was therefore not considered likely to have a major impact on measured dose for the majority of readings, and would therefore be adequately encompassed within the 5% error assigned.

Figure 1. Experimental set-up for assessment of out-of-field dose. Perspex slice holding chamber was substituted for various slices in the RANDO® phantom (The phantom Laboratory, USA).

2.5. Assessment of head leakage and scatter

To assess out-of-field dose due to head scatter and leakage, out-of-field chamber measurements were performed with the phantom pelvis (slices 30–35) removed, thus ensuring measured doses were predominantly from head scatter/leakage.

2.6. Second cancer risk evaluation

A variety of models exist for radiation-induced second cancer risk assessment, and the optimal is widely debated. Schneider's concept of OED (Schneider *et al* 2005, 2011), which incorporates the impact of fractionation, was adopted. This concept states that two different dose distributions which result in the same second cancer risk have the same OED. For higher dose in-field and close-to-field regions, where the dose–response is not considered linear, the OED concept was used to calculate risks of rectal and bladder cancer using:

(a) Schneider's mechanistic model (Schneider 2009), which includes tissue specific repair/ repopulation constants,
(b) a bell-shaped model (which suggests that risk increases in a linear fashion with dose up to a threshold before decreasing due to cell sterilization at higher doses without normal tissue repair (Schneider *et al* 2011), and
(c) a plateau model (which suggests that risk increases initially in a linear fashion as dose increases up to a threshold at which risk levels off due to cell sterilization at higher doses with full normal tissue repair (Schneider *et al* 2011).

The risks of radiation-induced pelvic bone and soft tissue second malignancies were calculated using a specific mechanistic sarcoma model (Schneider 2009).

Table 2. Parameters for RED and EAR calculations (Schneider *et al* 2011) and source of dosimetric data.

Site	Mechanistic model		Bell shaped model	Plateau model	β^a	γ_e (years)	γ_a (years)	Source of dose	Position of chamber from isocentre (cm)[b]
	α (Gy⁻¹)	R	α (Gy⁻¹)	α (Gy⁻¹)	(for calculation of EAR for mechanistic, bell-shaped, plateau and linear models)				
Rectum	0.033	0.56	0.031	0.065	0.73	−0.056	6.9	DVH	—
Bladder	0.219	0.06	0.213	0.633	3.8	−0.024	2.38	DVH	—
Pelvic bone sarcoma	Separate sarcoma model: $\alpha = 0.067$ based on intermediate repopulation ($R = 0.5$), $\beta^a = 0.20$					−0.013	−0.56	DVH	—
Pelvic soft tissue sarcoma	Separate sarcoma model: $\alpha = 0.060$, based on intermediate repopulation ($R = 0.5$), $\beta^a = 0.60$					−0.013	−0.56	DVH	—
Colon[c]	—	—	—	—	7.4	−0.056	6.9	Chamber	20[c]
Liver	—	—	—	—	2.4	−0.021	3.6	Chamber	25
Stomach	—	—	—	—	5.2	−0.002	1.9	Chamber	30
Lung	—	—	—	—	8.0	0.002	4.23	Chamber	Average of readings at 40 and 50
Oesophagus	—	—	—	—	3.2	−0.002	1.9	Chamber	Average of readings at 40, 50 and 60
Thyroid	—	—	—	—	0.40	−0.046	0.6	Chamber	60
Salivary glands	—	—	—	—	0.73	−0.024	2.38	Chamber	60
Mouth	—	—	—	—	0.73	−0.024	2.38	Chamber	65 (based on average of readings at 60 and 70)
Brain and CNS	—	—	—	—	0.70	−0.024	2.38	Chamber	70

[a] β: excess cases per 10 000 person-years gray, based on A-bomb survivors exposed at 30 years and surviving to 70 years, and modified for a UK population (see Schneider *et al* (2011) for further detail). Note this β is used for EAR calculation only. β within the α/β ratio is calculated from α based on $\alpha/\beta = 3$ Gy for all tissues.

[b] Positions of liver, stomach, thyroid and salivary glands based on work of Blais *et al* (2012).

[c] Point considered representative of dose received by transverse colon; DVH: dose–volume histogram.

Note: See text for explanation regarding α, R, β, γ_e and γ_a.

For low dose out-of-field regions, where dose–response is considered linear, the OED concept was used with a linear model.

The OED concept is discussed in detail elsewhere (Schneider *et al* 2005, 2011), but in summary:

$$\mathrm{OED} = \frac{1}{V_\mathrm{T}} \sum_i V_{D_i} \mathrm{RED}_{D_i}$$

where V_T is the total volume of the structure under consideration, V_D is the volume of the dose bin i which receives dose D_i and the RED_{D_i} is the risk equivalent dose for the dose bin receiving dose D_i. RED is calculated according to

(i) $\mathrm{RED}_D = \mathrm{D}$

when a linear model is applied (Schneider *et al* 2011), as is appropriate for low dose out-of-field regions
and

(ii) $\mathrm{RED}_D = \dfrac{e^{-\alpha' D}}{\alpha' R} \left(1 - 2R + R^2 e^{\alpha' D} - (1 - R)^2 \, e^{-\frac{\alpha' R}{1-R}D} \right)$

according to Schneider's mechanistic model which incorporates R, a tissue specific repair/repopulation parameter (Schneider *et al* 2011). The impact of fractionation here and in subsequent models is considered according to α' (Schneider *et al* 2011):

$$\alpha' = \alpha + \beta d = \alpha + \beta \frac{D}{D_T} d_T$$

where d is the dose per fraction, D_T is the dose prescribed to the target and d_T is the prescribed dose per fraction. Schneider *et al* fitted the parameters α and R for carcinoma induction using data from Atomic bomb survivors and patients treated with radiotherapy for Hodgkin disease (Schneider *et al* 2011). β is such that $\alpha/\beta = 3\,\mathrm{Gy}$.

To illustrate the possible OED in the extreme scenarios of no repair/repopulation, and full repair/repopulation, RED and thus OED can also be calculated according to

(iii) $\mathrm{RED}_D = D \exp(-\alpha' D),$

a bell-shaped model ($R = 0$) (Schneider *et al* 2011)
and

(iv) $\mathrm{RED}_D = \dfrac{1 - \exp(-\alpha' D)}{\alpha'},$

a plateau model ($R = 1$) (Schneider *et al* 2011).

All of the above models approach a linear model at low doses (Schneider *et al* 2011).

When considering radiation-induced sarcoma, RED is calculated as (Schneider *et al* 2011)

$$\mathrm{RED} = \frac{e^{-\alpha' D}}{\alpha' R} \left(1 - 2R + R^2 e^{\alpha' D} - (1 - R)^2 \, e^{-\frac{\alpha' R}{1-R}D} - \alpha' RD \right).$$

RED was also used to calculate the EAR of developing a radiation-induced second cancer in an organ with volume V_T after exposure to dose RED at one age (agex) and after attaining a greater age (agea), according to (Schneider *et al* 2011)

$$\mathrm{EARorg} = \frac{1}{V_T} \sum_i V_{D_i} \cdot \mathrm{RED}_{D_i} \cdot \beta \cdot \mu(\mathrm{agex},\mathrm{agea})$$

Table 3. MUs required for delivery of whole treatment course for the six radiation techniques delivered to the RANDO phantom (all from one patient).

Technique	Number of MUs for whole treatment course
SABR FFF	13 446
SABR	13 010
VMAT 78 Gy FFF	25 775
VMAT 78 Gy	24 040
IMRT 78 Gy	13 623
3D-CRT 78 Gy	10 429

where β is the initial slope for the dose–response curve for radiation-induced second cancers, V_D is the volume of the DVH bin receiving dose D_i, RED_{D_i} is the RED for that bin and μ is a modifying factor which adjusts for age at exposure (agex) and attained age (agea), calculated according to (Schneider *et al* 2011)

$$\mu \, (\mathrm{agex}, \ \mathrm{agea}) = \exp \left(\gamma_e \, (\mathrm{agex} - 30) \ + \ \gamma_a \times \ \ln \, (\mathrm{agea} \, / \, 70) \ \right)$$

where γ_e and γ_a are age modifying factors and where β was originally defined for persons exposed at age 30 years and attaining age 70 years.

All EAR calculations in this study were performed for patients irradiated at age 60 years and attaining age 80 years. All parameters for second cancer risk calculation were taken from (Schneider *et al* 2011) and are shown in table 2.

Doses and risks presented are those for the whole treatment course.

3. Results

3.1. Plans

The number of monitor units (MU) required for all fractions in the delivered plans are shown in table 3.

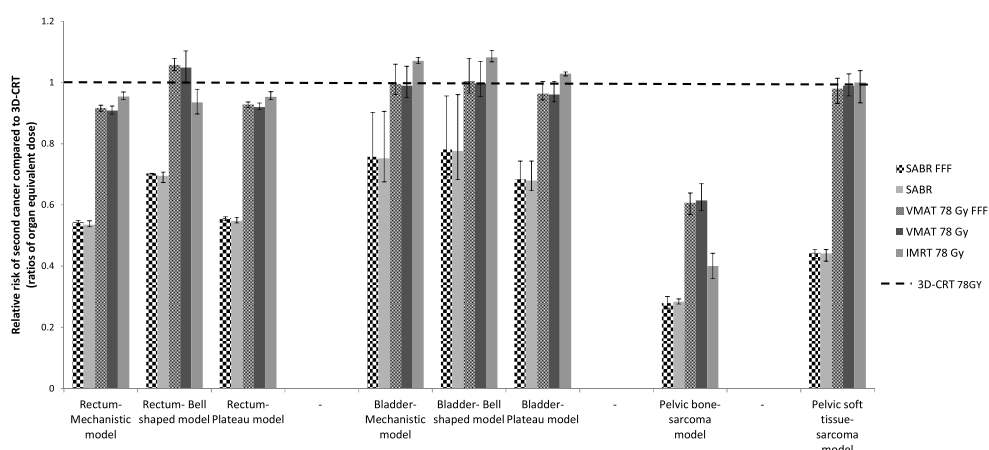### 3.2. In-field or close-to-field second cancer risks

Ratios of OED, thus relative risks of second rectal and bladder cancers and pelvic bone and soft tissue sarcoma for each technique relative to 3D-CRT, and averaged over the three evaluated pelvic CT scans, are shown in figure 2.

SABR techniques, both FFF and flattened, resulted in the lowest OEDs for in-field and close-to-field tissues, and thus resulted in the greatest risk reductions relative to 3D-CRT, regardless of the model used.

Considering all alternative 78 Gy techniques relative to 3D-CRT, and all models, relative risks of rectal cancer, bladder cancer or soft tissue sarcoma were within 9%, 8% and 2% of that for 3D-CRT respectively. Risk of bone sarcoma was lower using all alternative techniques compared to 3D-CRT.

When comparing FFF with the equivalent flattened technique, for in-field and close-to-field tissues, there was minimal difference in risk (average relative risks for FFF consistently within 2% of flattened techniques).

The EAR for in-field or close-to-field radiation-induced second cancer was low for all techniques and models (figure 3). Rectal and bladder cancer EARs ranged from 1.44–2.69

Figure 2. Relative risks of second malignancy in in-field or close-to-field tissues relative to 3D-CRT for whole treatment course. Error bars display the range of relative risks for the three pelvic CT scans used for planning.

and 1.70–2.42 per 10 000 persons per year (PY) respectively using the mechanistic model. Within each model, absolute differences between techniques were low, at most 1.25 and 0.96 per 10 000 PY for rectal and bladder cancer respectively. For each in-field or close-to-field site, absolute differences between models were also low, at most 1.09 per 10 000 PY for the rectum, and 0.66 per 10 000 PY for the bladder.

When comparing only 78 Gy techniques, absolute differences between techniques were small, at most 0.25 and 0.19 per 10 000 PY for rectal and bladder cancer respectively.

### 3.3. Out-of-field second cancer risks

Figure 4 shows radiation-induced second cancer risks relative to 3D-CRT (linear model).

As for in-field or close-to-field tissues, SABR resulted in reduced relative radiation-induced second cancer risks in out-of-field organs.

In contrast to in-field or close-to-field tissues, FFF in comparison to the equivalent flattened technique, resulted in relative radiation-induced second cancer risk reductions in out-of-field organs. The impact of FFF increased at greater distances from the treatment field. For example, in the region of the stomach, SABR FFF resulted in a 20% risk reduction relative to SABR, and VMAT 78 Gy FFF resulted in a 19% risk reduction relative to VMAT 78 Gy. In the region of the brain, both SABR FFF and VMAT 78 Gy FFF resulted in 56% risk reductions relative to equivalent flattened techniques.

In all out-of-field organs, IMRT resulted in increased radiation-induced second cancer risks relative to 3D-CRT, although increases were frequently small. At most, 26% risk increases were observed in the salivary gland and thyroid region using IMRT relative to 3D-CRT. Similarly, VMAT 78 Gy resulted in increased second cancer risks in most out-of-field organs of up to 55% relative to 3D-CRT. In contrast, VMAT 78 Gy FFF resulted in reduced second cancer risks relative to 3D-CRT of up to 32%.

EARs for second cancers in out-of-field organs were low for all sites and techniques (figure 5). At greater distances from the field, where the relative impact of FFF was greatest, in absolute terms, risks were very small. For example, in the region of the brain, the 56% risk reduction observed for FFF relative to the equivalent flattened technique, corresponded
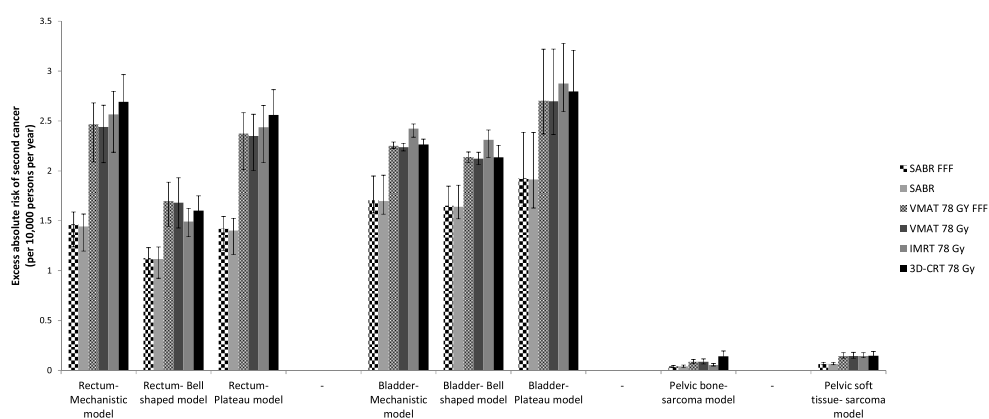
Figure 3. EARs of second malignancy in in-field or close-to-field tissues for whole treatment course based on patients being irradiated aged 60 and attaining 80 years. Error bars display the range of relative risks for the three pelvic CT scans used for planning.
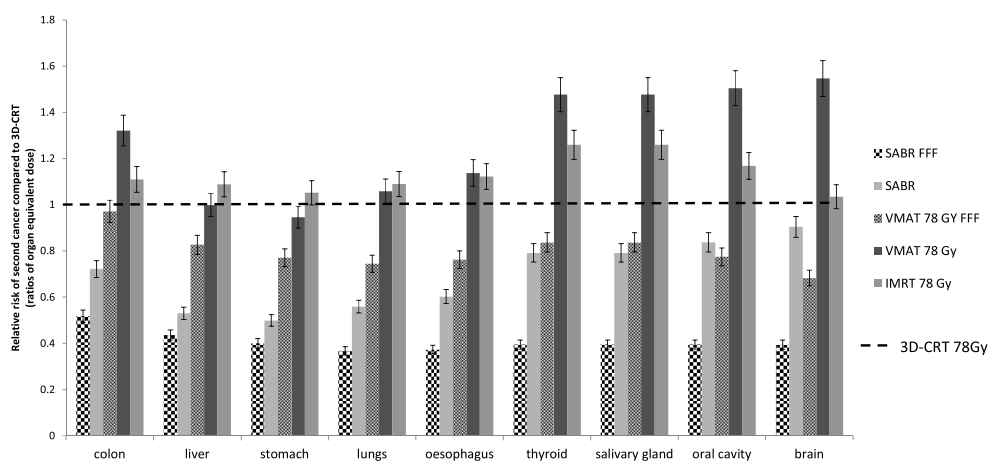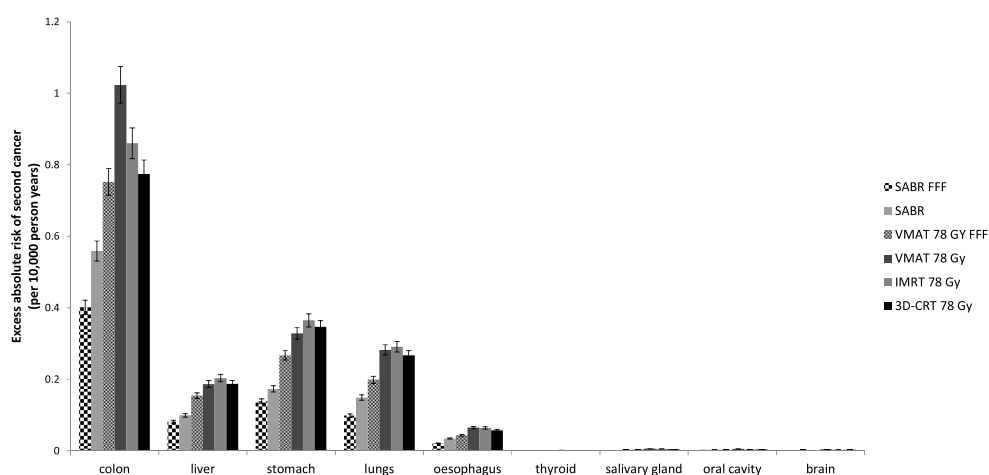

Figure 4. Relative risks of second malignancy in out-of-field tissues relative to 3D-CRT for whole treatment course. 5% error bars are shown to account for dosimetric and positioning uncertainty.

to absolute reductions from 0.0041 to 0.0018 per 10 000 PY for VMAT 78 Gy versus VMAT 78 Gy FFF and 0.0024 to 0.0011 per 10 000 PY for SABR versus SABR FFF, thus highlighting the fact that when absolute risks are very low, large relative risks become less relevant.

In absolute terms, the increased risk from IMRT relative to 3D-CRT was also small: the 26% relative risk increase corresponded to an EAR increase from 0.0041 to 0.0051 per 10 000 PY for 3D-CRT versus IMRT for salivary gland cancer, and from 0.0009 to 0.0011 per 10 000 PY for thyroid cancer. Similarly the 55% risk increase from VMAT 78 Gy relative to 3D-CRT, amounted to absolute increases from 0.0027 to 0.0041 per 10 000 PY for cancers of the brain respectively. The 32% risk reduction observed with VMAT 78 Gy FFF relative to 3D-CRT was also small in absolute terms (0.0027 to 0.0018 per 10 000 PY for second brain cancers). Thus this data also illustrate that large relative risks become unhelpful when absolute risks are very low.

Combining all the out-of-field EARs, plus EARs for pelvic bone and soft tissue sarcoma, as well as the highest average EAR from each of the three models used for second rectal and

Figure 5. EARs of second malignancy in out-of-field organs (linear model) for whole treatment course based on patients being irradiated aged 60 and attaining 80 years. 5% error bars are shown to account for dosimetric and positioning uncertainty.

bladder cancer estimation, the total EAR for a second cancer in any of the evaluated organs is shown for each technique in figure 6.

Thus SABR FFF resulted in the lowest 'total' second cancer risk (4.24 per 10 000 PY), and IMRT resulted in the highest 'total' second cancer risk (7.44 per 10 000 PY), thus the largest difference between techniques was low at 3.2 per 10 000 PY. The absolute differences between VMAT 78 Gy FFF, VMAT 78 Gy, IMRT 78 Gy and 3D-CRT were very low, at most 0.62 per 10 000 PY.

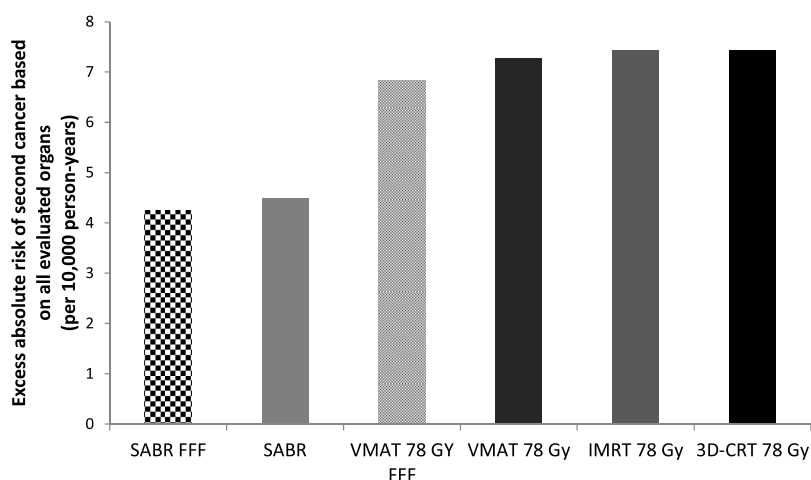### 3.4. Dose from head scatter and leakage

Out-of-field measurements performed following removal of the phantom pelvis demonstrated that FFF resulted in reduced out-of-field doses due to head scatter/leakage compared to equivalent flattened techniques. The proportion of dose resulting from head leakage/scatter is shown in figure 7.

### 3.5. Components of dose and distance

Changes in total dose, head leakage/scatter and within patient scatter (total dose minus head leakage/scatter) with distance are shown in figure 8. A slight increase in dose from within patient scatter was observed with FFF compared to the equivalent flattened beam at 10 and 15 cm from the isocentre, but this was outweighed by the reduction in dose due to reduced head leakage/scatter with FFF, resulting in lower total doses with FFF compared to the equivalent flattened technique. Beyond 15 cm from the isocentre, within patient scatter was similar between FFF and the equivalent flattened techniques.

4. Discussion

We aimed to assess radiation-induced second cancer risk following modern, clinically relevant prostate radiotherapy techniques. For all techniques, EARs were low. SABR conferred a consistently lower second cancer risk in all organs, while FFF conferred lower second cancer

Figure 6. Summed EAR for all evaluated organs for all techniques based on patients being irradiated aged 60 and attaining 80 years.
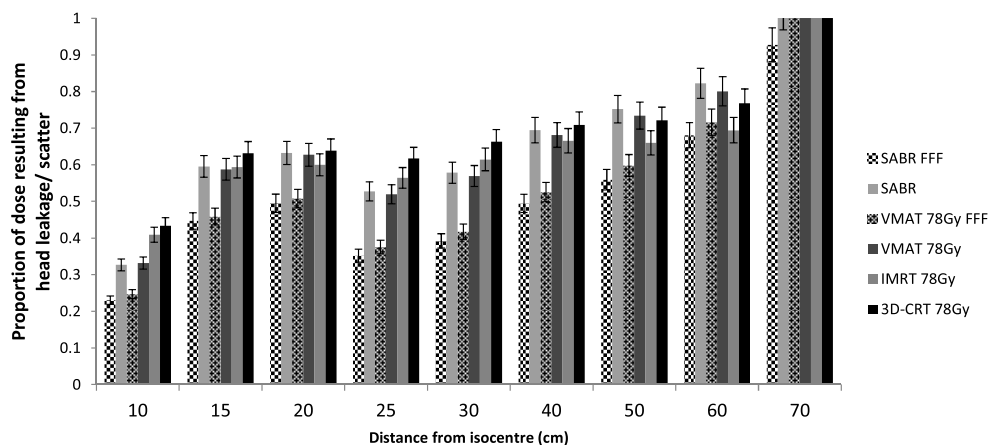

Figure 7. Proportion of out-of-field dose resulting from head leakage and head scatter. 3D-CRT: three-dimensional conformal radiotherapy, FFF: flattening filter free, 5% error bars are shown to account for dosimetric and positioning uncertainty.

risks in out-of-field organs, with the greatest relative impact at increasing distances from the field, where absolute benefits were small. The very low calculated absolute risks highlight the importance of not considering relative risks in isolation but also considering the associated absolute risks, as where absolute risks are very small, relative risks become far less important.

Prostate SABR delivers lower physical doses compared to conventionally fractionated treatments. Both lower physical doses and hypofractionation contributed to the observed second cancer risk reductions. The rationale for hypofractionation resulting in reduced second cancer risk has been discussed elsewhere (Schneider *et al* 2010).

While other groups have also observed the relative impact of FFF on out-of-field doses in prostate cancer (Kry *et al* 2010, Halg *et al* 2012), we are unaware that others have quantified the size of the benefit or assessed risk in the setting of energy-matched FFF and standard (flattened) beams. As above, it is clinically relevant to consider relative risks alongside
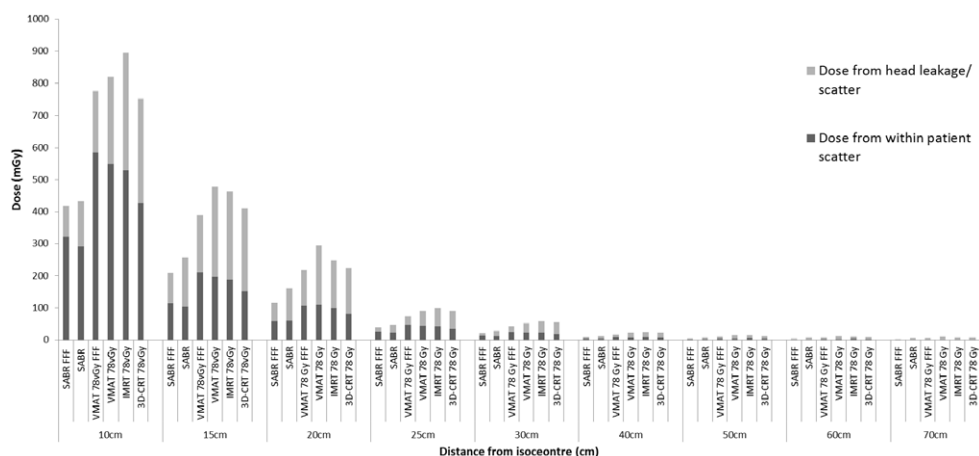
Figure 8. Changes in dose and components of dose with distance. 3D-CRT: three-dimensional conformal radiotherapy, FFF: flattening filter free, VMAT: volumetric modulated arc therapy.

corresponding absolute risks, although it is acknowledged that calculation of EAR, as an extension of OED calculation, introduces additional uncertainties (i.e. the steepness of the initial portion of the dose–response curve and adjustment for the age of the population in question). Despite this, calculated absolute benefits from FFF at large distances from the isocentre, were very small for this population. Irradiation of younger patients would result in greater absolute benefits from FFF. Most prostate cancer patients are, however, in the age range we considered, making calculated EARs relevant for the majority.

Kry *et al* (2010) evaluated non-energy matched FFF beams. An increase in total out-of-field dose was observed 3–15 cm from the field edge which was attributed to lower energy FFF photons resulting in increased within patient scatter, potentially increasing second cancer risks (Kry *et al* 2010). Using energy-matched FFF beams, we observed no such increase in total out-of-field dose, and the slight increase in within patient scatter was outweighed by the substantial reduction in head leakage/scatter.

Few groups have evaluated radiation-induced second cancer risk in prostate cancer from SABR (Dasu *et al* 2011) and VMAT (Rechner *et al* 2012). Comparisons with data from other groups are difficult because of the different methods employed. In addition, whole body risk is often calculated rather than individual organ risks. The impact of linac based SABR techniques on second malignancy risk has not been widely examined and we are aware of only one other group which has investigated this (Dasu *et al* 2011). Dasu *et al* quantified risks of second rectal and bladder cancer following 42.7 Gy in 7 fractions and 78 Gy in 39 fractions, both delivered using 3D-CRT (Dasu *et al* 2011). Exported DVHs were used to calculate risks using the competition model. Overall predicted risks were low, and CTV-PTV margin size had a larger impact on risk than fractionation schedule. The group concluded that the risks of second rectal and bladder cancers were similar between conventionally fractionated and ultra-hypofractionated regimens (Dasu *et al* 2011). Thus the potential in-field benefits of SABR that we observed in this study were not observed in Dasu *et al*'s work. This likely reflects the differences in the modelling processes used: the competition model used predicts a maximum second cancer effect at around 4 Gy, while according to the OED model and accompanying parameters, risks may become maximal at higher doses (see below). In addition, while both models incorporate fractionation, fractionation is incorporated into each model differently.

Table 4. Predicted percentage risks (%) of second rectal and bladder cancers based on competition model averaged for three pelvic CT scans

	Rectum		Bladder	
	Average	Range	Average	Range
SABR FFF	0.57	0.55–0.59	0.22	0.20–0.25
SABR	0.58	0.55–0.61	0.22	0.20–0.25
VMAT 78 Gy FFF	0.58	0.54–0.64	0.25	0.24–0.26
VMAT 78 Gy	0.58	0.55–0.63	0.25	0.24–0.26
IMRT 78 Gy	0.54	0.51–0.61	0.27	0.24–0.29
3D-CRT 78 Gy	0.47	0.43–0.55	0.25	0.22–0.27

Recalculating the risk of second bladder and rectal cancers for the three prostate patients using the competition model, and the same parameters as used by Dasu *et al*, we also observed broadly similar risks of second cancers between hypofractionated and all conventionally fractionated techniques (table 4). Reaching a definitive conclusion about which of the two models is more accurate is difficult, if not impossible.

There is epidemiological evidence which suggests that following irradiation for prostate cancer most second cancers arise in regions which receive doses greater than 5 Gy, thus including the rectum and bladder, and so adding support to Schneider's model (Berrington de Gonzalez *et al* 2011). Similarly, data from patients irradiated for cervical cancer has suggested that there is an increasing dose–risk relationship for second rectal and bladder cancer for doses up to 60 Gy and greater (Boice *et al* 1988). In contrast, however, it has been demonstrated that the dose–risk relationship for second rectal and bladder cancers following irradiation for a variety of primary tumour sites is essentially flat from doses of 1 to 60 Gy (Suit *et al* 2007), and other work, also following irradiation of a variety of primary tumour sites, has demonstrated that most second tumours arise at the edge of the PTV (Epstein *et al* 1997, Dorr and Herrmann 2002), which, in one of these studies, corresponded with regions receiving 6 Gy or less (Dorr and Herrmann 2002). No one model of radiation-induced carcinogenesis has ever been shown to be a perfect match for the epidemiological data, and epidemiological data, at times, appears conflicting. It is perhaps best, therefore, to view the differing results from the OED concept and competition model as illustrations of the uncertainties associated with the radiation-induced second cancer risk calculation process.

Few groups have evaluated radiation-induced second cancer risk in prostate cancer following VMAT compared to other external beam photon techniques. Rechner *et al* (2012) however, principally compared risks of bladder and rectal second cancer risks from VMAT with proton arc therapy. Excess relative risks were calculated and ratios of excess relative risks were used for comparisons (another modelling process which incorporates the effects of fractionation and reports risk relative to that in an non-irradiated population (Sachs and Brenner 2005, Shuryak *et al* 2009a, 2009b)). DVH data provided details of the therapeutic dose for VMAT and were also used to estimate secondary radiation doses (i.e. dose resulting from head leakage and scatter and additional within patient scatter). Monte Carlo simulations and previously published data were used to estimate secondary radiation doses resulting from proton arc therapy. Proton arc therapy predicted significantly lower risks of second bladder or rectal cancer according to linear-exponential and linear-plateau models compared to VMAT, while there was no significant difference in second rectal or bladder cancer risk when using the linear model. The group also compared calculated excess relative risks of second bladder and rectal from VMAT with that previously estimated for IMRT by

another group (Fontenot *et al* 2009). Numerically, VMAT resulted in lower risks of second bladder and rectal cancer compared to IMRT (excess relative risk for bladder cancer: 5.25 with VMAT and 8.88 with IMRT, excess relative risk for rectal cancer: 2.09 with VMAT and 3.32 for IMRT) (Rechner *et al* 2012). These risks, however, were calculated using a linear model, which is often considered inappropriate in higher dose regions (Hall and Wuu 2003, Ruben *et al* 2008). The use of a different model may also explain why greater differences were observed between IMRT and VMAT by Rechner *et al* and were greater than what was observed in this current piece of work.

Theoretical concerns have been raised regarding a potential large increase in second cancer risk using IMRT compared to 3D-CRT (Followill *et al* 1997, Hall and Wuu 2003, Kry *et al* 2005a, 2007, Stathakis *et al* 2007). Recent papers have suggested that any increased risk from 6 MV IMRT would be very small, particularly when compared to higher energy 3D-CRT (as often employed clinically) (Ruben *et al* 2008, 2011, Bednarz *et al* 2010, Ardenfors *et al* 2014). The theoretical risk increase is often attributed to two things: increased MU requirements for IMRT, resulting in increased head leakage, thus contributing to out-of-field dose, and the change in dose distribution, resulting in an increased volume of normal tissue receiving low doses. We observed increased risks from 6 MV IMRT and VMAT 78 Gy relative to 10 MV 3D-CRT in out-of-field organs of up to 26% and 55% respectively, likely because of increased MU. In absolute terms, however, where the greatest relative risk increases occurred, absolute increases were very small. VMAT 78 Gy FFF, however, resulted in reduced risks relative to 3D-CRT, although, again, absolute differences in risk were low. When considering individual in-field or close-to-field tissues, the impact of a change in dose distribution when moving from 3D-CRT to IMRT did not translate into clinically relevant increases in second cancer risk according to the models employed here. This can be explained through inspection of the DVHs for in-field and close-to-field organs. DVHs for all 78 Gy treatments for one pelvic CT are plotted in figures 9(*a*)–(*d*). The relationship between dose and risk equivalent dose (RED) according to Schneider's models has also been superimposed onto the DVH curves (Schneider *et al* 2011). Note that the values for RED are not shown, but the dose–RED curves are plotted purely to illustrate the shape of the dose–risk relationship.

Visual inspection of differential DVHs for the rectum for all 78 Gy treatments (figure 8(*a*)) are not suggestive that the rectum receives a greater proportion of low dose irradiation with IMRT, and dose distributions are largely similar between 3D-CRT and IMRT until around 40 Gy where there is a peak in the 3D-CRT DVH. For IMRT a smaller peak is seen around 48 Gy. In Schneider's model for rectal cancer induction, and based on the fractionation used here (i.e. 39 fractions), the risk peaks at about 23 Gy according to the bell-shaped model, and at about 35 Gy according to the mechanistic and plateau models. The 40–50 Gy region is therefore in the region of decreasing risk and the 48 Gy peak in the IMRT DVH falls in a lower risk portion of the curve compared to the 40 Gy peak for the 3D-CRT curve, and this may contribute to the slightly reduced risk observed in the risk of rectal cancer using IMRT relative to 3D-CRT (although in absolute terms the difference in risk is very small). Considering the VMAT treatments, a higher proportion of rectal tissue receives doses in the 15 to 25 Gy range compared to IMRT and 3D-CRT. This dose region falls in the highest risk portion of the bell-shaped model, thus resulting in the slightly increased risk of rectal cancer using VMAT relative to 3D-CRT and IMRT using this model. Considering the competition model, which predicts maximum effect at around 4 Gy, IMRT and VMAT treatments display a slightly higher volume of tissue receiving doses in the 3–4 Gy region, resulting in the slightly higher risks seen with IMRT and VMAT according to this model (table 4).

In the case of the bladder DVHs (figure 8(*b*)), IMRT appears to result in a slight increase in the volume of tissue receiving 2–5 Gy, which encompasses the area of maximal effect
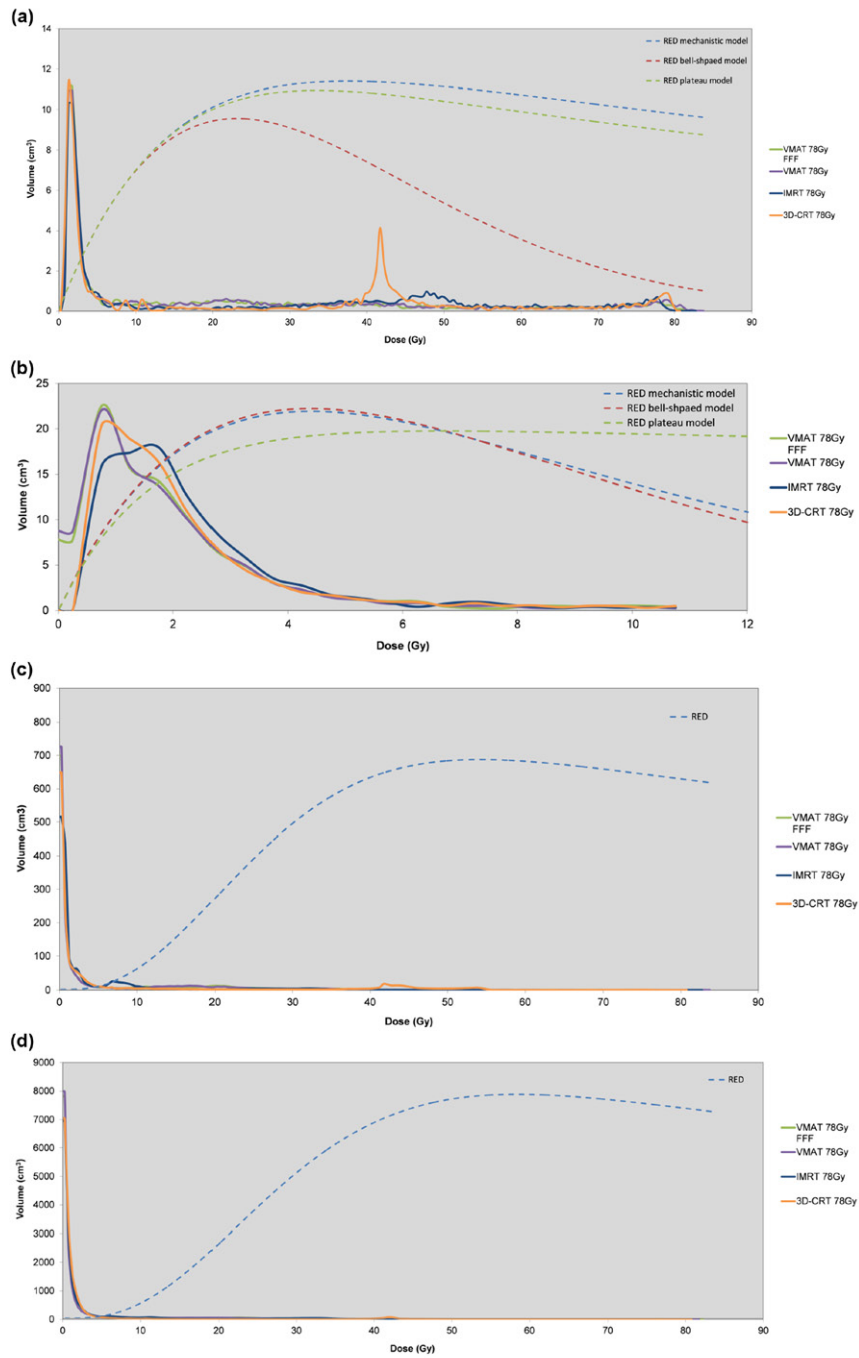
Figure 9. (*a*) Differential DVHs comparing 78 Gy techniques: rectum; RED: risk equivalent dose. (*b*) Differential DVHs comparing 78 Gy techniques: bladder (only first 10.5 Gy shown to allow differences to be more clearly observed); RED: risk equivalent dose. (*c*) Differential DVHs comparing 78 Gy techniques: pelvic bones; RED: risk equivalent dose. (*d*) Differential DVHs comparing 78 Gy techniques: pelvic soft tissues; RED: risk equivalent dose.

according to Schneider's bladders models, thus resulting in the slightly higher relative risk of second bladder cancers from IMRT compared to 3D-CRT. For both VMAT treatments, a smaller volume of tissue receives doses in the region of 1–2 Gy compared to 3D-CRT, and similar volumes of tissues receive doses of 3–5 Gy compared to 3D-CRT, thus resulting in only very slight second bladder cancer risk reductions using VMAT. These differences in dose distributions between techniques also explain the slight increase in second bladder cancer risk observed using IMRT compared to 3D-CRT, and similarities in risk between VMAT and 3D-CRT, according to the competition model.

Considering the pelvic bone DVHs (figure 8(*c*)), VMAT results in a larger volume of tissue receiving very low doses (<1 Gy) and IMRT results in a slight increased volume of tissue receiving doses around 2 Gy and around 6–10 Gy compared to 3D-CRT. Schneider's model, however, predicts a peak in bone sarcoma risk at around 54 Gy. A peak in dose is seen for the 3D-CRT plan at just above 40 Gy, thus falling in the higher risk region of the dose–RED curve, and contributing to the increased relative risk of second bone sarcoma observed for 3D-CRT compared to all other techniques, while the increased volume of bone receiving lower doses from IMRT and VMAT fall on a much lower risk part of the dose–risk curve, and thus have little impact on the calculated risk.

In terms of the soft tissue DVHs (figure 8(*d*)), where perhaps one might expect to see the biggest impact of an increased volume of tissue receiving a lower dose of radiation with IMRT or VMAT techniques, it can be seen that VMAT, as with the pelvic bone DVHs, results in a higher volume of tissues receiving very low doses (i.e. <1 Gy), while 3D-CRT results in a slightly larger volume of tissue receiving 2–3 Gy. Schneider's model predicts maximum effect at around 58 Gy and so it is doses in this region which will have the largest impact on risk. In the 50–60 Gy region, the DVH is largely similar for all techniques, and there is only a very slight peak at about 42 Gy for 3D-CRT. Overall, therefore, calculated risks for pelvic soft tissue sarcoma are similar for all four techniques, and the traditional concern that IMRT/VMAT techniques result in a larger volume of normal tissue receiving lower (and thus more cancer inducing) doses appears to contribute little to the overall calculated risk, according to the model used here.

The rectal, bladder, pelvic bone and pelvic soft tissue DVHs for the SABR FFF and standard (flattened) plans were very similar (data not shown), thus explaining the similar second cancer risks estimations for these two techniques, regardless of whether the OED concept or competition model was used.

There are a number of limitations in our work. Firstly, as alluded to above, there are uncertainties in radiation-induced second cancer models and parameters. Schneider's concept of OED was employed as this incorporates fractionation and, with the mechanistic model, includes repair and repopulation (Schneider *et al* 2011). Models based on full and no repair/repopulation, were also adopted to illustrate a range of possibilities. All models suggested benefit from SABR in in-field or close-to-field tissues, which is where the majority of radiation-induced second cancers arise (Epstein *et al* 1997, Dorr and Herrmann 2002, Berrington de Gonzalez *et al* 2011). Similarly, all models predicted broadly comparable second rectal and bladder cancer risks from 3D-CRT, 5-field IMRT and VMAT 78 Gy (FFF or standard).

Secondly, the appropriateness of these linear-quadratic (LQ) based models for high dose per fraction treatments could be questioned (Brenner 2008, Kirkpatrick *et al* 2008). Our SABR prescription dose was 6.1 Gy per fraction, and, most normal tissues received doses far below the prescription dose. Where concern about high dose per fraction treatments and the LQ model have been raised, this is usually in the setting of radiosurgical doses (e.g. >10 Gy per fraction) (Kirkpatrick *et al* 2008). Thus the doses considered in this current study were within the range in which the LQ model is considered reliable.

Thirdly, we did not assess the impact of neutron contamination on second cancer risks for the 10 MV plan. It has previously been demonstrated, however, that at 10 MV this effect is very small (Kry *et al* 2005a). Fourthly, only three patients' pelvic CT scans were evaluated for in-field and close-to-field second cancer risks, and only one was evaluated for out-of-field risks. Similar to this study, the majority of prostate cancer planning studies which evaluate radiation-induced second cancer risks in a series of adult patients, all planned using the same variety of techniques, do so in one to three patients. The reason for the small sample size is that the primary interest is differences between techniques rather than inter-patient variability (Kry *et al* 2005b, 2010, Schneider 2006, Stathakis *et al* 2007, Ruben *et al* 2008, Fontenot *et al* 2009, Bednarz *et al* 2010, Kragl *et al* 2011, Blais *et al* 2012, Rechner *et al* 2012) A few studies have, however, compared up to 10 patients, each planned using the same variety of techniques (Fontenot *et al* 2010, Patil *et al* 2010, Yoon *et al* 2010). Dasu *et al* (2011), however, aimed to evaluate inter-patient variability in second cancer risk and so included 100 patients, each planned using SABR and conventionally fractionated radiotherapy, although this analysis was restricted to rectal and bladder DVH analysis, and did not include out-of-field dose measurements. Given the relative anatomical constancy of the prostate in relation to organs-at-risk, however, any variability in second cancer risk is likely to be less than what might be expected for tumours with greater variability in location, suggesting that a low number of patients may be acceptable. This is reinforced by the consistency in results for the three evaluated patients, thus adding confidence to our use of a small patient sample. For out-of-field organs, minimal variation in dose between patients would be expected, and so the use of one patient, planned in several different ways, is adequate for comparison of different techniques.

We did not include the impact of image-guided radiotherapy (IGRT) on second cancer risk as this will vary with the IGRT technique employed. The CTV–PTV margin was intended for daily online IGRT with fiducial markers. Thus conventionally fractionated regimens will require at least 39 images while SABR will require at least 7 images. If automatic couch adjustments are used, and treatment is sufficiently rapid, then further imaging following shifts or post-treatment would be unnecessary. The need for fewer images with ultra-hypofractionated regimens potentially adds additional second cancer benefit to SABR techniques.

Different hardware and software combinations as well as treatment margins may all contribute to differences in second cancer risk (Ruben *et al* 2008, Dasu *et al* 2011). We attempted to minimize these as far as possible by delivering all plans on the same machine, by creating plans using the same planning system as far as possible, and by using the same CTV–PTV margin. Differences in risks observed in this study should therefore largely be due to the doses, fractionations and planning techniques under evaluation. Our findings are, however, specific for the planning and delivery systems adopted here.

5. Conclusion

In summary, we compared radiation-induced second cancer risks following contemporary clinically relevant radiotherapy techniques for early prostate cancer. SABR resulted in reduced relative second cancer risks in all organs, while FFF resulted in reduced second cancer risks in out-of-field organs relative to equivalent flattened techniques, particularly at greater distances from the treatment field. Although large differences in relative risk were sometimes observed, in absolute terms, second cancer risks were low, emphasizing the importance of considering absolute risks in addition to the comparison of relative risks. Until clinical data regarding

radiation-induced second cancers in irradiated prostate patients treated with contemporary techniques matures, data from this and other planning studies should be considered when selecting appropriate radiation techniques for individual patients.

Conflicts of interest

Acknowledgments

References

Adamson J, Wu Q and Yan D 2011 Dosimetric effect of intrafraction motion and residual setup error for hypofractionated prostate intensity-modulated radiotherapy with online cone beam computed tomography image guidance *Int. J. Radiat. Oncol. Biol. Phys.* **80** 453–61

Ardenfors O, Josefsson D and Dasu A 2014 Are IMRT treatments in the head and neck region increasing the risk of secondary cancers? *Acta Oncol.* **53** 1041–7

Bednarz B, Athar B and Xu X G 2010 A comparative study on the risk of second primary cancers in out-of-field organs associated with radiotherapy of localized prostate carcinoma using Monte Carlo-based accelerator and patient models *Med. Phys.* **37** 1987–94

Beltran C, Herman M G and Davis B J 2008 Planning target margin calculations for prostate radiotherapy based on intrafraction and interfraction motion using four localization methods *Int. J. Radiat. Oncol. Biol. Phys.* **70** 289–95

Berrington de Gonzalez A, Curtis R E, Kry S F, Gilbert E, Lamart S, Berg C D, Stovall M and Ron E 2011 Proportion of second cancers attributable to radiotherapy treatment in adults: a cohort study in the US SEER cancer registries *Lancet Oncol.* **12** 353–60

Blais A R, Lederer E, Oliver M and Leszczynski K 2012 Static and rotational step-and-shoot IMRT treatment plans for the prostate: a risk comparison study *Med. Phys.* **39** 1069–78

Boice J D Jr *et al* 1988 Radiation dose and second cancer risk in patients treated for cancer of the cervix *Radiat. Res.* **116** 3–55

Brenner D J 2008 The linear-quadratic model is an appropriate methodology for determining isoeffective doses at large doses per fraction *Semin. Radiat. Oncol.* **18** 234–9

Dasu A, Toma-Dasu I, Franzen L, Widmark A and Nilsson P 2011 Secondary malignancies from prostate cancer radiation treatment: a risk analysis of the influence of target margins and fractionation patterns *Int. J. Radiat. Oncol. Biol. Phys.* **79** 738–46

Dearnaley D P 2010 *CHHiP Trial Protocol: Conventional or Hypofractionated High Dose Intensity Modulated Radiotherapy for Prostate Cancer* Protocol version 9, Protocol number: ICR-CTSU/2006/10007 (http://public.ukcrn.org.uk/search/StudyDetail.aspx?StudyID=1281)

Dorr W and Herrmann T 2002 Second primary tumors after radiotherapy for malignancies: treatment-related parameters *Strahlenther. Onkol.* **178** 357–62

Epstein R, Hanham I and Dale R 1997 Radiotherapy-induced second cancers: are we doing enough to protect young patients? *Eur. J. Cancer* **33** 526–30

Fiorino C, Valdagni R, Rancati T and Sanguineti G 2009 Dose–volume effects for normal tissues in external radiotherapy: pelvis *Radiother. Oncol.* **93** 153–67

Followill D, Geis P and Boyer A 1997 Estimates of whole-body dose equivalent produced by beam intensity modulated conformal therapy *Int. J. Radiat. Oncol. Biol. Phys.* **38** 667–72

Fontenot J D, Bloch C, Followill D, Titt U and Newhauser W D 2010 Estimate of the uncertainties in the relative risk of secondary malignant neoplasms following proton therapy and intensity-modulated photon therapy *Phys. Med. Biol.* **55** 6987–98

Fontenot J D, Lee A K and Newhauser W D 2009 Risk of secondary malignant neoplasms from proton therapy and intensity-modulated x-ray therapy for early-stage prostate cancer *Int. J. Radiat. Oncol. Biol. Phys.* **74** 616–22

Franzen L and Widmark A 2011 *HYPO-RT-PC Trial Protocol. Phase III Study of Hypofractionated Radiotherapy of Intermediate Risk Localised Prostate Cancer* Version 6.0. ISRCTN45905321 (www.controlled-trials.com/ISRCTN45905321)

Halg R A, Besserer J and Schneider U 2012 Systematic measurements of whole-body dose distributions for various treatment machines and delivery techniques in radiation therapy *Med. Phys.* **39** 7662–76

Hall E J and Wuu C S 2003 Radiation-induced second cancers: the impact of 3D-CRT and IMRT *Int. J. Radiat. Oncol. Biol. Phys.* **56** 83–8

Huang J, Kestin L L, Ye H, Wallace M, Martinez A A and Vicini F A 2011 Analysis of second malignancies after modern radiotherapy versus prostatectomy for localized prostate cancer *Radiother. Oncol.* **98** 81–6

Kirkpatrick J P, Meyer J J and Marks L B 2008 The linear-quadratic model is inappropriate to model high dose per fraction effects in radiosurgery *Semin. Radiat. Oncol.* **18** 240–3

Kragl G, Baier F, Lutz S, Albrich D, Dalaryd M, Kroupa B, Wiezorek T, Knoos T and Georg D 2011 Flattening filter free beams in SBRT and IMRT: dosimetric assessment of peripheral doses *Z. Med. Phys.* **21** 91–101

Kry S F, Followill D, White R A, Stovall M, Kuban D A and Salehpour M 2007 Uncertainty of calculated risk estimates for secondary malignancies after radiotherapy *Int. J. Radiat. Oncol. Biol. Phys.* **68** 1265–71

Kry S F, Salehpour M, Followill D S, Stovall M, Kuban D A, White R A and Rosen Ii 2005a The calculated risk of fatal secondary malignancies from intensity-modulated radiation therapy *Int. J. Radiat. Oncol. Biol. Phys.* **62** 1195–203

Kry S F, Salehpour M, Followill D S, Stovall M, Kuban D A, White R A and Rosen Ii 2005b Out-of-field photon and neutron dose equivalents from step-and-shoot intensity-modulated radiation therapy *Int. J. Radiat. Oncol. Biol. Phys.* **62** 1204–16

Kry S F, Vassiliev O N and Mohan R 2010 Out-of-field photon dose following removal of the flattening filter from a medical accelerator *Phys. Med. Biol.* **55** 2155–66

Patil V M, Kapoor R, Chakraborty S, Ghoshal S, Oinam A S and Sharma S C 2010 Dosimetric risk estimates of radiation-induced malignancies after intensity modulated radiotherapy *J. Cancer Res. Ther.* **6** 442–7

Paynter D, Weston S J, Cosgrove V P, Evans J A and Thwaites D I 2014 Beam characteristics of energy-matched flattening filter free beams *Med. Phys.* **41** 052103

Quon H, Loblaw D A, Cheung P C, Holden L, Tang C, Pang G, Morton G, Mamedov A and Deabreu A 2012 Intra-fraction motion during extreme hypofractionated radiotherapy of the prostate using pre- and post-treatment imaging *Clin. Oncol.* **24** 640–5

Radiation Therapy Oncology Group 2014 *RTOG 0126 Trial Protocol: A Phase III Randomized Study of High Dose 3D-CRT/IMRT Versus Standard Dose 3D-CRT/IMRT in Patients Treated for Localised Prostate Cancer* Version June 2014 (www.rtog.org/ClinicalTrials/ProtocolTable/StudyDetails. aspx?study=0126)

Rechner L A, Howell R M, Zhang R, Etzel C, Lee A K and Newhauser W D 2012 Risk of radiogenic second cancers following volumetric modulated arc therapy and proton arc therapy for prostate cancer *Phys. Med. Biol.* **57** 7117–32

Ruben J D, Davis S, Evans C, Jones P, Gagliardi F, Haynes M and Hunter A 2008 The effect of intensity-modulated radiotherapy on radiation-induced second malignancies *Int. J. Radiat. Oncol. Biol. Phys.* **70** 1530–6

Ruben J D, Lancaster C M, Jones P and Smith R L 2011 A comparison of out-of-field dose and its constituent components for intensity-modulated radiation therapy versus conformal radiation therapy: implications for carcinogenesis *Int. J. Radiat. Oncol. Biol. Phys.* **81** 1458–64

Sachs R K and Brenner D J 2005 Solid tumor risks after high doses of ionizing radiation *Proc. Natl Acad. Sci. USA* **102** 13040–5

Schneider U 2006 Calculated risk of fatal secondary malignancies from intensity-modulated radiotherapy: in regard to Kry *et al* (letter) *Int. J. Radiat. Oncol. Biol. Phys.* **64** 1290

Schneider U 2009 Mechanistic model of radiation-induced cancer after fractionated radiotherapy using the linear-quadratic formula *Med. Phys.* **36** 1138–43

Schneider U, Besserer J and Mack A 2010 Hypofractionated radiotherapy has the potential for second cancer reduction *Theor. Biol. Med. Model.* **7** 4

Schneider U, Sumila M and Robotka J 2011 Site-specific dose–response relationships for cancer induction from the combined Japanese A-bomb and Hodgkin cohorts for doses relevant to radiotherapy (and associated erratum) *Theor. Biol. Med. Model.* **8** 27

Schneider U, Zwahlen D, Ross D and Kaser-Hotz B 2005 Estimation of radiation-induced cancer from 3D dose distributions: concept of organ equivalent dose *Int. J. Radiat. Oncol. Biol. Phys.* **61** 1510–5

Shuryak I, Hahnfeldt P, Hlatky L, Sachs R K and Brenner D J 2009a A new view of radiation-induced cancer: integrating short- and long-term processes: I. Approach *Radiat. Environ. Biophys.* **48** 263–74

Shuryak I, Hahnfeldt P, Hlatky L, Sachs R K and Brenner D J 2009b A new view of radiation-induced cancer: integrating short- and long-term processes: II. Second cancer risk estimation *Radiat. Environ. Biophys.* **48** 275–86

Stathakis S, Li J and Ma C C 2007 Monte Carlo determination of radiation-induced cancer risks for prostate patients undergoing intensity-modulated radiation therapy *J. Appl. Clin. Med. Phys.* 8 (www.jacmp.org/index.php/jacmp/article/view/2685/1351)

Suit H, Goldberg S, Niemierko A, Ancukiewicz M, Hall E, Goitein M, Wong W and Paganetti H 2007 Secondary carcinogenesis in patients treated with radiation: a review of data on radiation-induced cancers in human, non-human primate, canine and rodent subjects *Radiat. Res.* **167** 12–42

Yoon M, Ahn S H, Kim J, Shin D H, Park S Y, Lee S B, Shin K H and Cho K H 2010 Radiation-induced cancers from modern radiotherapy techniques: intensity-modulated radiotherapy versus proton therapy *Int. J. Radiat. Oncol. Biol. Phys.* **77** 1477–85

Zelefsky M J *et al* 2012a Incidence of secondary cancer development after high-dose intensity-modulated radiotherapy and image-guided brachytherapy for the treatment of localized prostate cancer *Int. J. Radiat. Oncol. Biol. Phys.* **83** 953–9

Zelefsky M J, Pei X, Teslova T, Kuk D, Magsanoc J M, Kollmeier M, Cox B and Zhang Z 2012b Secondary cancers after intensity-modulated radiotherapy, brachytherapy and radical prostatectomy for the treatment of prostate cancer: incidence and cause-specific survival outcomes according to the initial treatment intervention *BJU Int.* **110** 1696–701